Contents lists available at ScienceDirect

Biomedical Signal Processing and Control

journal homepage: www.elsevier.com/locate/bspc

# Combinational spectral band activation complexity: Uncovering hidden neuromuscular firing dynamics in EMG

Nicholas J. Napoli [a,f,*], Anthony R. Mixco [b], Savannah V. Wooten [c], Marco Jacopetti [d], Joseph F. Signorile [e]

[a] Dept. of Electrical and Computer Engineering, University of Florida, Gainesville, FL 32611, United States
[b] Dept. of Environmental &Radiological Health Sciences, Colorado State University, Ft. Collins, CO80526, United States
[c] Division of Pediatric Research, University of Texas M.D. Anderson Cancer Center, Houston, TX, 77030, United States
[d] Dept. of Neuroscience, University of Hospital of Modena, Modena, Italy
[e] Dept. of Kinesiology and Sports Sciences, University of Miami, Coral Gables, Fl 33146, United States
[f] Human Informatics and Predictive Performance Optimization (HIPPO) Laboratory, University of Florida, Gainesville, FL 32611, United States

ARTICLE INFO

*Keywords:*
Electromyography (EMG)
Entropy
Wavelets
Muscle Fiber Type Changes
Age Related Neuromuscular Firing Dynamics
Conduction Velocity
Fiber Typing
Isometric Contractions
Plantar Flexion
Dorsiflexion
EMG Complexity
Geriatrics

ABSTRACT

A new approach, Combinational Spectral Band Activation Complexity (CSB-AC), that extracts the neuromuscular firing dynamics of surface electromyography (sEMG) signals by applying entropic methods in a multi-dimensional fashion by analyzing the signals temporally, spectrally, and intensity dynamics simultaneously is presented. The CSB-AC signal processing approach introduces a methodology that highlights that a small amount of key fiducial points embedded within the sEMG, 1000x reduction in EMG data, are only needed to show statistically significant changes of the neuromuscular firing dynamics.

CSB-AC was compared to the more generalized sample entropy method to demonstrate physiological differences between cohorts and baseline mapping between the two measurements. Results indicated significant differences between CSB-AC and sample entropy regardless of age groups for tibialis anterior and plantar flexion muscles (gastrocnemius medialis, gastrocnemius lateralis, and soleus). Significant differences were found between older and younger subject groups for the gastrocnemius medialis and soleus with the older adults having higher complexity values. CSB-AC produces greater complexity than sample entropy, where this sparser set of data holds paramount information for describing neuromuscular firing and should not be ignored. CSB-AC, accomplishes this by simultaneously assessing the complexity of sEMG's time, intensity, and spectral content, where latent properties of neuromuscular dynamics within this unique set of sparse sEMG data points are critical to characterizing neuromuscular firing.

## 1. Introduction

This paper presents a new signal processing method, Combinational Spectral Band Activation Complexity (CSB-AC), which is designed to provide insights into the complex nature of modulated firing of muscle fibers. This new surface electromyographic (sEMG) approach has the potential to further explain changes to the underlying neuromuscular dynamics that occur within aging, diseased and injured populations. sEMG is the accepted standard for measuring muscle activity [1]; however, sEMG produces nonlinear, electrical signals created by the superposition of action potentials from hundreds to thousands of motor units. Surface electrodes capture magnitude (recruitment) and density (firing frequency) of motor units dictated by the electrodes size and configuration. The recruitment of motor units and changes in conduction velocity of the nerve are super-imposed at the surface electrode. This superposition convolves the signals between individual motor unit activations and their associated spectral properties, making it difficult to understand the neuromuscular dynamics involved. The problem of deconvolving or demodulating the signal is further complicated by standard bi-polar surface electrodes since their distances from the motor end plates vary, causing phasic shifts in signal from fibers with the same conduction velocities to be super-imposed within the sEMG

* Corresponding author.
*E-mail addresses:* n.napoli@ufl.edu (N.J. Napoli), Anthony.Mixco@colostate.edu (A.R. Mixco), svwooten@mdanderson.org (S.V. Wooten), Jacopetti.marco@aou.mo.it (M. Jacopetti), jsignorile@miami.edu (J.F. Signorile).

https://doi.org/10.1016/j.bspc.2021.102891
Received 8 September 2020; Received in revised form 31 May 2021; Accepted 16 June 2021

measurement. These global complex firing patterns occurring (synchronously and asynchronously) could be loosely conceptualized as an orchestra with instruments playing various frequencies at distinct times as dictated by the piece. Therefore, CSB-AC, is designed to demodulate the signal by capturing the entropic nature of how frequencies are activated as a function of time.

**Prior Work:** To address these complexities, researchers have developed intricate and costly electrode topology to deconvolve these modulated signals [2]; however, these designs require highly expensive and complex data acquisition systems, which are not available to the average clinician and researcher. From a signal analysis perspective, researchers have developed an assortment of signal processing techniques. Tscharner demonstrated that in order to appropriately analyze discrete events, an intensity measure was needed that provided time resolution that could distinguish between single events, while preserving spectral content [3]. Intensity analysis with non-linearly scaled wavelets has also become a common sEMG [4–11] and mechanomyography [12–15] analysis technique. Although this intensity measure can allow unique comparisons of individual spectral temporal events, there is additional information within the sEMG that is not revealed because of the signal modulation and sEMG non-linear complexities. Most recently, entropic analysis techniques have been used to measure the complexity of sEMG [16–20].

However, these applied entropy methods strictly analyze the temporal dynamics and capture only non-linear changes as a function of time. As there are abrupt non-linear sEMG magnitude changes within the time series (which can be attributed to changes in motor unit recruitment and conduction velocity), the entropy measurements are able to capture and quantify these dynamics [17–20]. When an abrupt increases in the magnitude of the sEMG time series occurs, an increase of the modulated spectral waveforms (e.g motor unit action potentials, conduction velocity. and etc.) are embedded. These embedded spectral waveforms that compose the sEMG are not being accounted for using the available entropy approaches and the true temporal dynamics of these spectral waveforms within the time domain are unknown. Therefore, the activation of these spectral waveforms that are modulated go unnoticed and unmeasured because they are embedded within the sEMG signal (see Fig. 1).

This raises one fundamental research question about neuromuscular firing dynamics that have never been seen before. If we decompose these embedded spectral waveforms as a function of time and intensity, does the arrival times (using the fiducial marker as the peak intensity) of these spectral waveforms during a contraction statistically differentiate between two cohorts known to have different neuromuscular firing patterns.

**Challenges:**

As discussed earlier, the two components that drive frequency content within the sEMG can be thought of as sections of an orchestra where we have dozens of instruments playing simultaneously. Additionally, as sEMG has been described as linearly enveloped Gaussian distribution [8], rather than hearing the instruments playing together, instead each instrument is playing a different song and all that is heard is noise.

From a data collection and experimental perspective, sEMG data spectra and intensity can be influenced by the type of muscle contraction. Although isotonic and isokinetic contractions can be appropriate when measuring power [21,22], they can affect the sEMG signal negatively as the contractions require the muscles to change length. The rate at which the muscle changes length influences the spectra. This can also cause additional vibrational noise that could be added to the sEMG signal. Furthermore, isokinetic and isotonic contractions have two phases, concentric and eccentric, as the muscles begin at rest, go to a minimum length, and return to rest. Napoli [8] reported that for the vastus lateralis, vastus medialis, and rectus femoris, the concentric loading phase had significantly higher intensity levels than the eccentric loading phase through multiple frequency bands.

**Insight:** Due to spectral modulation that drives the sEMG signal, there are no methods that are able to decode a signal collected using a bipolar configuration; however, it may be possible to draw insight from these neuromuscular dynamics by quantifying how non-linear temporal dynamics change as a function of frequency content of the sEMG signal. Again our orchestra analogy can be employed. An orchestra can play components of a song, where there is a harmony and a melody. The harmony may be composed of many notes (frequency information) and the melody is the timing of the notes (timing information). By examining the exact instance in time a note (frequency) is played, we can characterize the harmony and melody. However, it is not entirely possible to pin-point the exact frequency and the time the notes occur because of the Heisenberg uncertainty principle [8]. In addition, a sEMG signal's frequency information can't be contextually summarized into a band-limited frequency (i.e., an exact frequency like a musical note). No physical meaning of a sEMG band-limited frequency has ever actually been achieved (such as fiber typing with sEMG); however, untenable suggestions have been made [23–26]. From this body of work, if arbitrary assumptions regarding frequency band information are made, we could use these to evaluate a signal's complex structure based upon modulation of the sEMG signal. Such a pseudo-modulation approach can then be applied to conditions, physiological cohorts, and demographic cohorts that have previously characterized neuromuscular firing

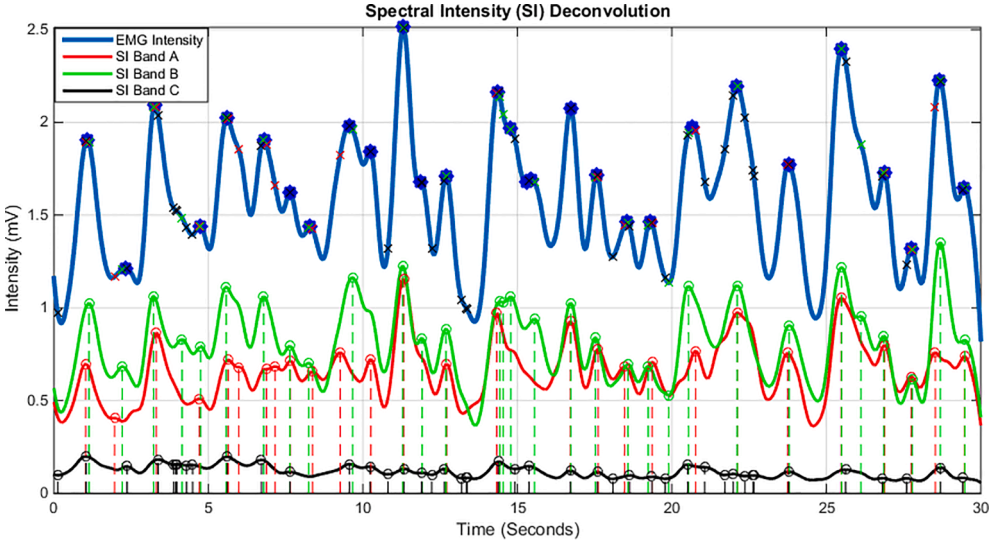


**Fig. 1.** This simulated sEMG figure demonstrates how an sEMG's intensity (in blue) can change over time and how an sEMG can be deconvolved into its embedded spectral intensity (SI) bands (in green, red and black). The SI bands can be determined through the wavelet intensity methodology [3,8] that is used in this paper. The sEMG signal's peak intensity occurs when there is maximum activation, highlighted with the blue dots. However, we observe that as the sEMG signal is deconvolved the timing of the activation across the SI bands differ temporally. This is highlighted with vertical lines that connect with the peaks of each of the SI band time series. The different activation across the SI bands are then hidden within the complete "EMG Intensity" waveform.

dynamics to understand the advantages and discriminative capacity such a method would provide.

We hypothesize that such an approach can be achieved through three milestones: *(1) Decomposing the signal into its frequency components as a function of time (e.g., the types of musical notes); (2) depicting the activation or instance of these frequencies (e.g., the timing of intensity of the musical notes); and (3) quantifying the structure and pattern of these neuromuscular firing dynamics.* The first milestone can be accomplished by applying a wavelet intensity analysis to the sEMG signal, which will decompose the signal into different frequency bands [3,8]. When the intensity of the wavelet band peaks (maximizes), we will assume that to be a time specific instance to complete the second milestone. Lastly, the use of complexity measurements can provide the framework for quantifying the structure of the signal predictability, completing the third milestone. The greater the complexity of the signal, the more irregular and unpredictable the time series will be [17]. Electrophysiological signals such as sEMG, EEG, and ECG signals have been analyzed with entropy measures [18,27–30] to explain particular changes in complexity of the signals. However, using entropy measures such as approximate entropy, Shannon entropy, or fuzzy entropy only provide analysis of the time domain and ignore the spectral domain. The spectral content is lost along with the information held within its medium. However, by applying the first and second milestones to the analysis, spectral content could be preserved through use of a time–frequency analysis prior to examining complexity. With that, more could be learned about the signals themselves. Currently, only one paper has reported comparative rationale for decomposing the spectral intensity's activation to characterize neuro-firing, and this was utilized in electroencephalogram to characterize cognitive impairments [31]. However, this work merely isolates the spectral bands intensities and does not examine the impact of how these signals work together in describing neuronal firing.

From an experimental perspective, we can leverage the known impacts of aging on neuromuscular firing patterns to evaluate such a proposed novel algorithm. More specifically, unique patterns from the complexity analysis of surface electromyography have been examined with aging [30,32–34] indicating that a comparison between younger and older adults would be very appropriate for CSB-AC. Aging is a natural process that affects energy distribution into different frequency bands [35–43]. Specifically, decreases in muscle strength, power, and control occur as a result of aging [35,43–45].

## 2. Methods

### 2.1. Study design and data collection

#### 2.1.1. Participants

Thirty participants were placed into twos groups; young persons (Y) ages 20–25, and older persons (O) ages 60–79. The young group consisted of 10 participants and the elderly group consisted of 20 participants; each group was equally divided between male and female. Inclusion criteria stated that all participants must be healthy without any history of ankle injuries, uncontrolled neuromuscular, orthopedic, cardiovascular disease, or any other health-related circumstances that may have affected neuromuscular responses during testing. Following approval by University's Human Subject Research Internal Review Board, participants were recruited using flyers and University contacts.

#### 2.1.2. Procedures

All testing sessions took place at the Laboratory of Neuromuscular Research and Active Aging. Testing required a one time, 45 min, visit to the laboratory. Subjects signed all consent forms approved by the University's Subcommittee for the Use and Protection of Human Subjects, and were administered a general health questionnaire, and anthropomorphic measurements were taken. Subjects had their dominant leg prepared for surface electrode placement on the tibialis anterior (TA), peroneus longus (PL), gastrocnemius medialis (GM), gastrocnemius lateralis (GL), and soleus. To minimize signal interference, the surface of the subjects' skin was shaved, abraded, and cleansed with rubbing alcohol. Since placement of the electrodes on the muscle can affect the signal properties. Disposable Ag/AgCl dual electrodes (Noraxon USA, Inc., Scottsdale, AZ) were positioned parallel to the underlying muscle fibers according to Crams Introduction to Surface Electromyography [46].

#### 2.1.3. Testing

Following electrode placement, subjects performed a 60s plantar flexion (PF) and dorsiflexion (DF) maximal isometric contraction on the Biodex 4 Dynamometer (Biodex Inc., Shirley, New York). The subject was seated in the Biodex chair with their leg, ankle, and foot supported by an external attachment (Fig. 2). At a "go" cue, the subject either performed a perceived maximal isometric contractions at 5 degrees of PF or 25 degrees of DF. Participants were given verbal encouragement throughout all isometric contractions. Although PF and DF employ different muscle groups, a fifteen minute recovery was provided between the PF and DF isometric tests to reduce the impact of residual fatigue.

#### 2.1.4. Analysis

The Biopac 150 system (BIOPAC Systems Inc., Goleta, California) was used to collect and analyze EMG signals of the TA, PL, GM, and GL during isometric testing. The Biopac 150 system has an input impedance of 1.0 M and common mode rejection ratio (CMRR) of 110 dB min (50/60HZ). The gain was set at 1,000 with band pass filtering set between 20 and 450 Hz. Signals were sampled at a frequency of 1000 Hz, digitized using a 16-bit A/D converter and stored on a laptop laboratory computer. Recorded EMG signals from each muscle were analyzed using the Biopac 150 system software. Normalized root mean square EMG (Nrms EMG) was calculated during the maximum voluntary contraction (MVC) from the participants' initial 3-4s time interval.

### 2.2. Combinational spectral band activation complexity

#### 2.2.1. EMG wavelet intensity filtering

We utilized Von Tscharner's classical approach of intensity filter implementation [3]. His proposed wavelet basis function defined by,

$$\widehat{\psi}_i(fc_i, scale, f) = \left(\frac{f}{fc_i}\right)^{\eta} \cdot e^{\left(1-\frac{f}{fc_i}\right)\eta} \cdot \Theta(f) \tag{1}$$

where, $\eta = (fc_i \cdot scale), i \in \{1, \ldots, K\}$ filters, $fc$ is the center frequency of a particular wavelet, f is the range of frequencies, and $\Theta(f)$ is a heavy side function only expressing frequencies greater than zero. However, we deviated from the original methodology because of the valid concerns presented by Gabriel [47]. This discussion points out how applying the designed filters to the EMG's source signal in the frequency domain,

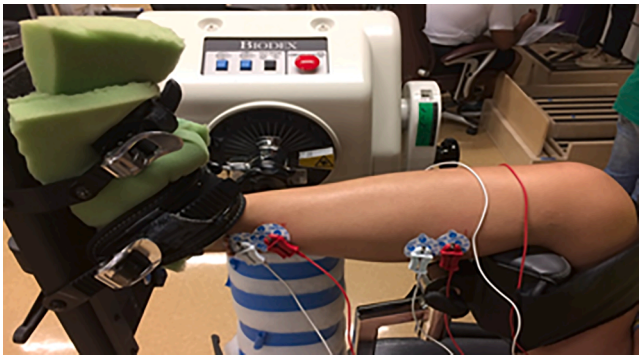

**Fig. 2.** The demonstrated isometric study design using the Biodex 4 Dynamometer.

$X_s(f)$, is inappropriate since we are applying the Fourier transform to a non-stationary signal, thus defeating one of the major purposes of the novel signal processing approach. As Borg highlights [48], von Tscharner's implementation shares similarities to a basic equalizer that decomposes the EMG time domain's source signal, $x_s(n)$, into its associated intensity components, $I_i(n)$, with respect to each filtering process, $\kappa_i$, shown in Fig. 3. This presented wavelet method convolves the sEMG time domain signal, $x_s(n)$, with the wavelet filter, $\widehat{\psi}_i(n)$ and Gaussian smoothing methods. We define this entire process as, $\widehat{\kappa}_i$, where $i \in \{1, \ldots, K\}$ filters.

In order to obtain $\widehat{\psi}_i(n)$, we transfer the designed respective frequency domain filter, $\widehat{\psi}_i(fc_i, a_i, b_i)$, to the time domain by,

$$\widehat{\psi}_i(n) = \mathscr{C}^{\mathscr{S}}\left\{\mathscr{F}^{-1}\left\{\widehat{\psi}_i(fc_i, a_i, b_i)\right\}\right\}, \tag{2}$$

where $\mathscr{F}^{-1}$ is the inverse Fourier transform and $\mathscr{C}^{\mathscr{S}}$ is the circular shift of the numeric output of the function, where $L = \frac{N}{2}$ and N is the length of the filter in the time domain. The $\mathscr{C}^{\mathscr{S}}$ operation with $L = \frac{N}{2}$ is equivalent to performing a FFT shift, which adjusts the mirroring image in the frequency domain. However, this sequence happens to be in the time domain. Thus, the sequence $\{x(0), \ldots, x(N-1)\}$ is cyclically shifted to $\{x(N/2), x(N-1), 0, \ldots, x(N/2-1)\}$. By applying the Eq. (2), we are able to move the filter designed in the frequency domain to the time domain described with real and imaginary components. Utilizing the filter in time domain, $\widehat{\psi}_i(n)$, we obtain the intensity of the signal $x_s(n)$, which is defined by the convolution of $x_s(n)$ with $\widehat{\psi}_i(n)$. The intensity sequence, $I_i(n)$, is then smoothed using a Gaussian filter,

$$G_f(n) = \frac{1}{\sqrt{2\pi\sigma^2}} e^{-0.5\left(\frac{x}{\sigma}\right)^2} \tag{3}$$

where $\sigma = \frac{F_s}{4}, F_s$ is the sampling frequency and $x = \in \left\{\frac{-3F_s}{4}, \ldots, \frac{3F_s}{4}\right\}$. The implementation of the smoothing is achieved by

$$\widehat{I}_i(n) = I_i\left(n\right) * G_f\left(n\right), \tag{4}$$

where we obtain a smoothed filtered intensity EMG sequence.

After completion of the wavelet intensity filtering, the sEMG sequence was divided into 6 equal length time segments (windows) before proceeding to the next analysis step. Each window segment was 10 s in length.

### 2.2.2. Activation sets

Activation Sets analysis is the second step in Fig. 3 that visually depicts the process for calculating CSB-AC. By first utilizing each smoothed filtered spectral intensity band, $\widehat{I}_i(n)$, a generalized peak detector, $\rho_t$, is applied to the time series. The peak detector, $\rho_t$, was the invoked function "findpeaks" from MatLab version 2017a. This MatLab function produces a vector of length, $J_i$, yielding the locations in time where the maximum intensity activates for a spectral band, $\widehat{\tau}_i$, where $i \in \{1, \ldots, K\}$ filters, each $J_i$ may not be equivalent, and $J \ll N$. Thus when a peak detector, $\rho_t$, is applied to a spectral intensity band, $\widehat{I}_i(n)$, we produce an Activation Set, $\widehat{\tau}_i$, which describes the timing of how that particular spectra's intensity activates. This process was completed for each of the 6 windows.

From the prospective of an orchestra playing components of a song, where there is a harmony and melody we attempt to capture the "melody" of the bio-signal by combining all of the activation sets back together into one temporal sequence. This is achieved by concatenating all the activation's sets, $\widehat{\tau}_C = [\widehat{\tau}_1, \widehat{\tau}_2, \ldots, \widehat{\tau}_k]$ and then applying a sort function to $\widehat{\tau}_C$ (in which only unique time instances are provided and no duplicated time instances are reported from other K sets). This concatenated and sorted sequence, $\widehat{A}_T$, denotes how various spectra intensify and dampen as a function time through the mixture of influences of spectral neuromuscular factors of conduction velocity and motor unit recruitment. This concatenated and sorted sequence, $\widehat{A}_T$, is defined by,

$$\widehat{A}_T = \left[a_1, a_2, a_3 \ldots, a_{T-1}, a_T\right], \tag{5}$$

where T is the total amount of intensity activation that occurred across all K filters and $T \ll L$.

### 2.2.3. Activation complexity

Although we captured the neuromuscular spectral temporal sequence, we have no quantitative way of evaluating this combined sequence of activation. Thus, we use the temporally combined activation sets, $\widehat{A}_T$, to examine the predictability of how intensity in a sequence, $\widehat{I}_i(n)$ changes. By examining the interval of times that occur between each activation, we can remove any mean off-set of the sequence across subjects and specifically look at the timing of the sequence. This is achieved by taking the difference of the vector $\widehat{A}_T$ and operationalized by,

$$\Delta\widehat{A}_T = \left[a_2 - a_1, a_3 - a_2, \ldots, a_T - a_{T-1}\right], \tag{6}$$

$$\Delta\widehat{A}_T = \left[A_1, A_2, \ldots, A_S\right], \tag{7}$$

where $A_i = a_{i+1} - a_i$ and $S = T - 1$. Following this, we process the entropy of the new sequence, $\Delta\widehat{A}_T$, with an entropic method to quantify the complexity of the activation. For this particular experimental case, sample entropy was applied [49]. A template vector with length $m$, where $A_m(i) = \{A_i, A_i + 1, \ldots, A_{i+m-1}\}$ and distance function $d[A_m(i), A_m(j)]_{(i \neq j)}$. Utilizing the template vector and distance function, we define sample entropy by,

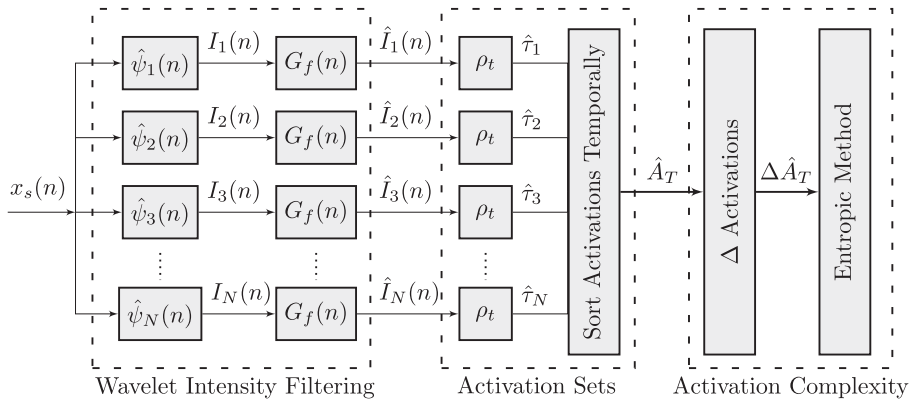


**Fig. 3.** A flow diagram describes the *Combinational Spectral Band Activation Complexity (CSB-AC)* method. The first part of the method, the wavelet intensity filtering, mimics an equalizer in which the input signal $x_s(n)$ is decomposed into their respective frequency and intensity components, $\widehat{I}_i(n)$, via the defined wavelets, $\widehat{\phi}_i(n)$. The next part of the process finds the time instances of when the intensity peaks or activates, across all $\widehat{I}_i(n)$ and sorts the instances as function of time. The last part of the process, Activation Complexity, computes the time intervals between the activations. Activation Complexity then examines the predictability of these activations via sample entropy.

$$SampEn\left(\Delta\widehat{A}_T, r, m\right) = -log\left(\frac{B}{C}\right), \tag{8}$$

where $B$ is the number of $d[A_m(i), A_m(j)] < r$, $C$ is the number of $d[A_{m+1}(i), A_{m+1}(j)] < r$, $m = 2$, and $r = .2 \cdot std(\Delta\widehat{A}_T)$. This reported entropy value from the sequence, $\Delta\mathbf{A}_T$ produced our Combinational Spectral Band Activation Complexity (CSB-AC). Again this process was completed for each window, yielding 6 CSB-AC values. It is important to note that the type of entropy measurement employed to the sequence will be sensitive to the number of data points in the sequence, thus limiting the window size that can be analyzed. Typically sample entropy and permutation entropy require a minimum of 100 samples, whereas approximate entropy requires a minimum of 1000 samples [27]. Based on the 10 s windowing scheme, we produced well over 100 samples for each widow (On average across all subjects there was an average of 161.88 ± 23.38 samples produced).

### 2.3. Statistical analysis

A 2 (technique) x 2 (age group) x 6 (window) mixed ANOVA was used to determine differences between age groups and sample entropy and CSB-AC processing techniques across six windows. When significant main effects or interactions were detected, least square differences (LSD) post hoc tests were used to determine the sources. All statistical analysis was performed using SAS 9.3 (IBM SAS Statistics, Cary, NC). Statistical significance was set a priori at $p < 0.05$.

## 3. Results

### 3.1. Sample entropy vs CSB-AC

Results of the mixed ANOVA for each muscle are presented below. Before moving forward, it is important to note that the variables $\eta$ from Eq. (1) and $\eta^2$ as seen below in the ANOVA results are completely unrelated.

#### 3.1.1. Tibialis anterior

For the TA, the repeated measures ANOVA revealed a significant effect by analysis method (Sample Entropy vs CSB-AC) ($p = .006$; $\eta^2 = .125$), and a significant Window x Group Interaction ($p < .0001$; $\eta^2 = .142$). Pairwise comparisons between analysis methods revealed that CSB-Activation Complexity produced significantly higher comp lexity than Sample Entropy ($M_{diff} = .199 \pm .070$; 95%$CI$: [.058, .340]; $p = .006$; $d = .73$). When groups were compared within windows, no significant difference was found between the younger and older adults for window one; however, significant differences were seen for all other windows with the older group producing higher intensity levels than the younger group (see Fig. 4). Pairwise comparisons examining the differences among windows within groups (see Fig. 5) revealed that for older individuals significant differences were seen among all win dows except for windows 3 and 4 ($M_{diff} = .038 \pm .028$; 95%$CI$ : [−.018, .940]; $p = .179$), 4 and 5 ($M_{diff} = .07 \pm .038$; 95%$CI$ : [−.018, .940] ; $p = .061$), and 5 and 6 ($M_{diff} = .043 \pm .035$; 95%$CI$ : [−.113, .027] ; $p = .223$).

A similar pattern (see Fig. 5) was seen for the younger subjects with significant differences observed between windows 1, 2, and 3; and these windows were significantly different than windows 4, 5 and 6. No differences were seen between windows 4, 5, and 6.

#### 3.1.2. Peroneus longus

The repeated measures ANOVA for the peroneus longus revealed a significant effect by Window ($p < .0001$; $\eta^2 = .457$) and a significant Group x Window interaction ($p < .0001$; $\eta^2 = .142$). Once again, the pairwise comparison between groups within each window showed no significant difference between the younger and older participants for window one; however, significant differences were seen for all other windows with the older group producing significantly higher complexity levels than the younger group (see Fig. 6). Pairwise comparisons examining the differences among windows within groups revealed that for older adults no significant differences were seen between windows 1 and 2, windows 3, 4 and 5, and windows 5 and 6. For the younger group, window 1, 2, and 3 were significantly different from all other windows while no significant differences were seen between windows 4 and 5, or windows 5 and 6 (see Fig. 7).

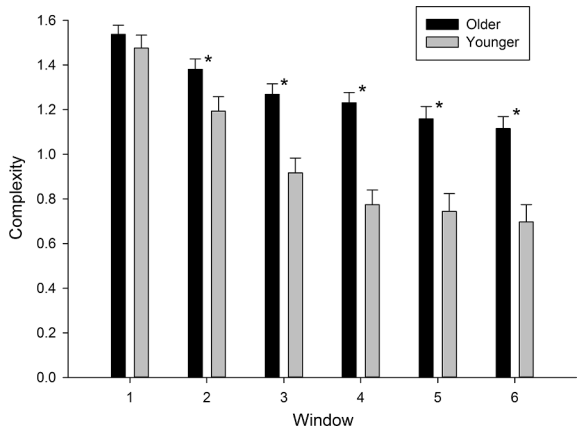


**Fig. 4.** Differences between the Younger and Older groups across windows for the Tibialis anterior.

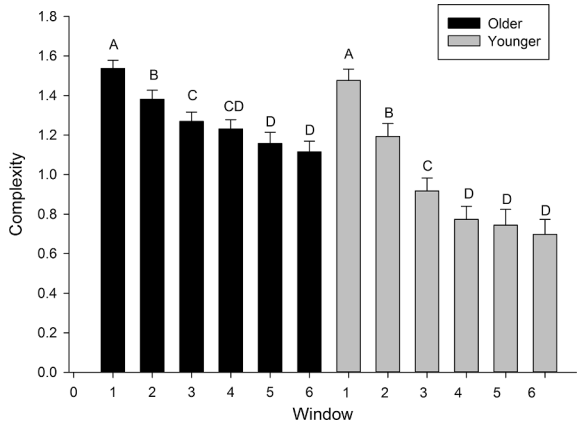


**Fig. 5.** Differences among windows for the older and younger groups for the Tibialis anterior. (Windows with the same letter are not significantly different from one another.)

#### 3.1.3. Soleus

For the Soleus, the mixed ANOVA revealed significant differences in complexity for Window ($p = .001$; $\eta^2 = .089$), Group ($p < .0001$; $\eta^2 = .119$), and Analysis Method ($p = .048$; $\eta^2 = .068$). Post hoc testing for group showed that older individuals produced more complexity than younger individuals ($M_{diff} = .303 \pm .081$; 95%$CI$ : [.140, .466]; $p < .0001$; $d = 1.02$), CSB-Activation Complexity produced significantly higher complexity than Sample Entropy ($M_{diff} = .164 \pm .081$; 95%$CI$ : [.001, .327]; $p = .048$; $d = .50$) (see Fig. 8), and no significant differences were seen between Window 1, 2, 3, 4, and 5, between Windows 4 and 5, or between Windows 5 and 6 (see Fig. 9).

#### 3.1.4. Gastrocnemius lateralis

The ANOVA for the gastrocnemius lateralis revealed a significant main effect by window ($p = .012$; $\eta^2 = .062$), a significant group x window interaction ($p = .004$; $\eta^2 = .076$), and a significant main effect

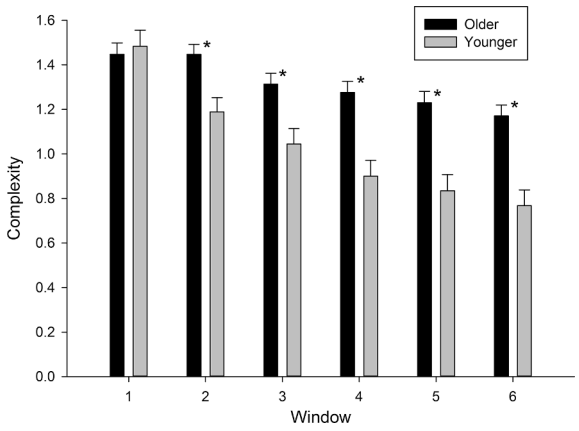


**Fig. 6.** Differences between the Younger and Older groups across windows for the Peroneus longus.

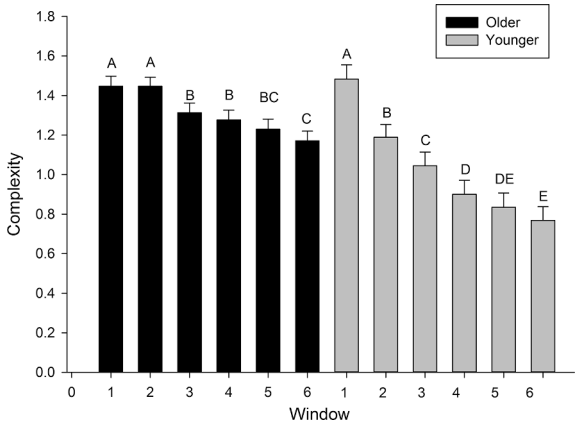


**Fig. 7.** Differences among windows for the older and younger groups for the Peroneus Longus. (Windows with the same letter are not significantly different from one another.)

by analysis method ($p < .0001$; $\eta^2 = .301$). The pairwise comparison for analysis method revealed that CSB-Activation Complexity produced significantly higher complexity than Sample Entropy ($M_{diff} = .384 \pm .078$; $95\%CI : [.227, .541]$; $p = .0001$; $d = 1.21$) (see Fig. 10). The

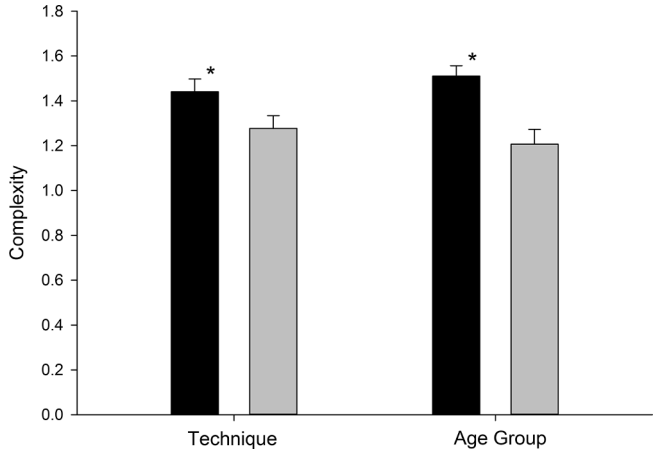


**Fig. 8.** Impacts of Technique (black bar = CSB-Activation Complexity; grey bar = Sample Entropy) and Age Group (black bar = Older; grey bar = younger) on complexity for the Soleus.*greater than Sample Entropy (Technique) or Younger Group (Age Group).

pairwise comparison between groups within each window showed significantly greater complexity for the older compared to the younger participants for windows 3, 4, and 6 (see Fig. 11). Pairwise comparisons evaluating differences among windows for older individuals revealed no significant differences between windows 1 and 2, windows 3, 4 and 5, and windows 5 and 6. For the younger group, significant differences were seen between window 1 and all other windows. However, no significant differences were found between windows 2, 3, 4, and 5; or between window 3, 4, 5, and 6 (see Fig. 12).

### 3.1.5. *Gastrocnemius medialis*

For the gastrocnemius medialis there were significant main effects for group ($p = .037$; $\eta^2 = .075$); analysis method ($p < .0001$; $\eta^2 = .482$); and window ($p = .038$; $\eta^2 = .045$). Pairwise comparisons for group showed that the older participants demonstrated significantly greater complexity than younger individuals ($M_{diff} = .155 \pm .073$; $95\%$ $CI : [.009, .301]$; $p = .037$; $d = .36$); while CSB-Activation Complexity produced significantly higher complexity than Sample Entropy ($M_{diff} = .526 \pm .073$; $95\%CI : [.380, .672]$; $p < .0001$; $d = 2.92$) (see Fig. 13). Post hoc analyses for window revealed that window 1 was not significantly different from any other window; while window 2 was not different from windows 3 and 4. Finally, window 4 was not different than window 5, and window 5 was not different than window 6 (see Fig. 14).

## 4. Discussion

Complexity is a numerical representation of the unpredictability and irregularity of a signal [16]. It can be calculated using different entropic measures such as approximate entropy, fuzzy approximate entropy, and sample entropy. Albeit these classical entropic measures have been used in the field of EMG signal analysis, they still require further validation to fully interpret how entropy can be applied to the interpretation of the EMG signal. This paper introduces the capacity of a novel method, CSB-AC, to provide insights into the mechanisms of modulating muscle firing patterns and further elucidate underlying neuromuscular dynamics. CSB-AC was compared to the sample entropy method in a sample of healthy younger and older men and women to assess differences in the methods' capacities to quantify muscle complexity during an isometric contraction. Surface EMG from five muscles were assessed.

### 4.1. *Tibialis anterior*

As part of the testing the subjects completed a 60s dorsiflexion maximal isometric contraction with the TA being the primary agonist.

The significantly greater values for CBS-AC vs sample entropy indicate a potentially greater sensitivity of the former to the underlying

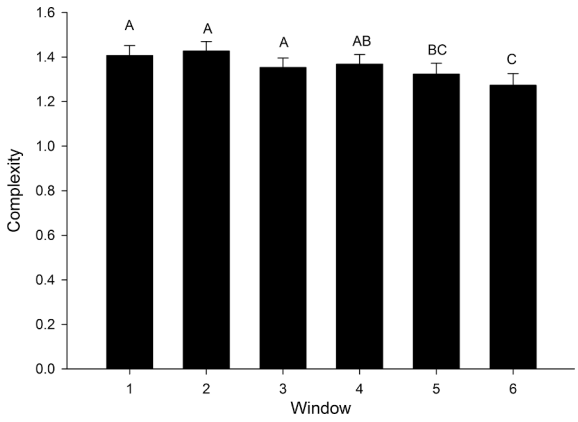


**Fig. 9.** Differences among windows for the Soleus across the entire sample. (Windows with the same letter are not significantly different from one another.)

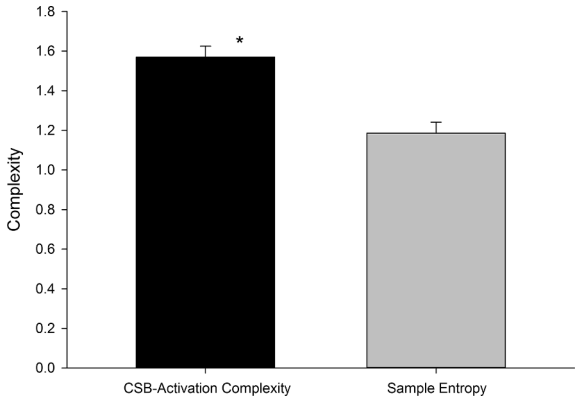


**Fig. 10.** Comparison of complexity assessment techniques for the Gastrocnemius Lateralis. (*Significantly greater than Sample Entropy, $p < .0001$).

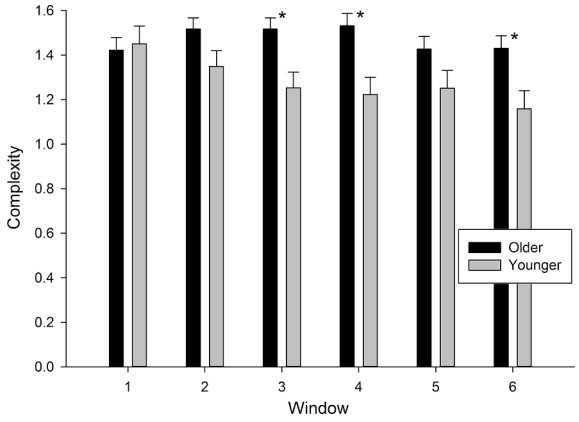


**Fig. 11.** Differences between the older and younger participant groups across windows for the Gastrocnemius Lateralis. (*Significantly higher than the younger group, $p < .009$).

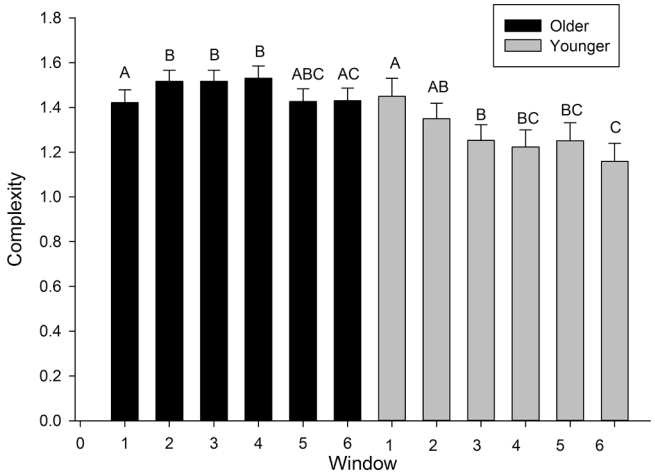


**Fig. 12.** Differences across windows within the older and younger groups for the Gastrocnemius Lateralis. (Windows with the same letter are not different from one another.)

neuromuscular factors within the sEMG signal. Since complexity is a representation of a signal's unpredictability and irregularity, a higher value may indicate more irregularity or unpredictability within the EMG signal. Alternatively, it could be postulated that the signal processing technique is capturing more noise; however, this is unlikely, as CSB-AC

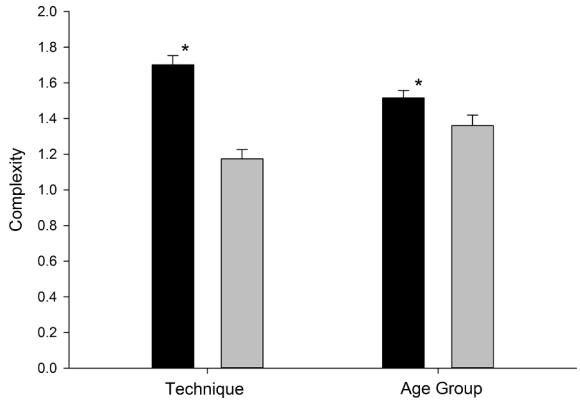


**Fig. 13.** Impacts of Technique (black bar = CSB-Activation Complexity; grey bar = Sample Entropy) and Age Group (black bar = Older; grey bar = younger) on complexity for the Gastrocnemius Medialis. (*greater than Sample Entropy (Technique) or Younger Group (Age Group)).

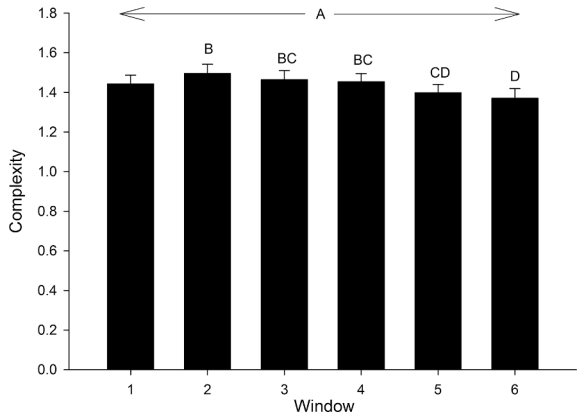


**Fig. 14.** Differences among windows for the Soleus across the entire sample. (Windows with the same letter are not different from one another.)

evaluates the overall signal size as it determines specific points in time that are associated with the location of maximum intensity. Therefore, this significant interaction supports the effectiveness of using CSB-AC when measuring sEMG complexity. When examining the window x group interaction, the pairwise comparison revealed that as the window increased, the complexity showed a significantly greater decrease in the younger adults than older adults (Fig. 4); however, both older and younger adults exhibited significant progressive decreases in patterns of complexity across windows (Fig. 5).

The similarity in decreasing complexity patterns was expected as higher window numbers reflect the later part of the contractions and muscle fatigue would be expected as the duration of the isometric contraction increased, regardless of the subjects' ages. However, the higher complexity observed in older adult windows was expected, as complexity represents increased unpredictability and chaos [50]. Further, the larger decreases in complexity seen in our younger versus older subjects may be reflective of the greater decreases in motor unit firing rates in the TA of younger than older persons during maximal isometric contractions [51].

### 4.2. Plantar flexors

Because the muscles of the triceps surae all contribute to plantar flexion, their results should be examined holistically. For the PL, the more rapid decrease in complexity levels by the younger subjects than their older counterparts across windows was not unexpected, given the similar pattern seen in the TA and the similarities in size and fiber

structure between the PL and TA.

For the Soleus, the significant main effects for Group, Window, and analysis method should be expected. Like the TA, the higher complexity values for CSB-AC than sample entropy may indicate the greater sensitivity of the CSB-AC to the factors affecting the sEMG signal (Fig. 8 left). Furthermore, the older adults had greater complexity numbers than the younger adults (Fig. 8 right) likely due to a more rapid fatigue-related decline in complexity across windows in the younger adults due to their high initial power outputs. However, this may not be evident given the fatigue resistant nature of the predominantly slow twitch Soleus and the lower magnitude of difference between groups.

The ANOVA analysis for the GL, which showed greater levels of complexity seen with CSB-AC compared to sample entropy, once again reflects the greater sensitivity of CBS-AC to the underlying neuromuscular factors within the sEMG signal (Fig. 10). However, when examining Window and Group x Window interaction the patterns differed somewhat from those seen in the previous muscles. The greater complexity values of the older compared to younger adults across windows 3, 4 and 6 (Fig. 11) and that their declines in complexity across windows was limited (Fig. 12), may reflect the fatigue resistance often reported in older compared to younger persons during maximal contractions [52,53].

As with the other muscles of the triceps surae, the higher complexity values for CSB-AC than sample entropy seen in the GM indicated its greater sensitivity to the changes in the components of the sEMG signal (Fig. 13 left). The older adults had greater complexity than the younger adults (Fig. 13) and the complexity levels showed little decline across windows. Like the Soleus, the greater complexity values and lesser decline in complexity values seen for the older group seen in the GM, likely reflects lower fatigue levels during the maximum voluntary contraction possibly mirroring the aforementioned fatigue resistance that accompanies aging [52,53] and the fiber type restructuring favoring Type I fibers evidenced during the aging process [54].

### 4.3. Interpretations

#### 4.3.1. Aging and complexity

As previously discussed, complexity is a numerical representation of the unpredictability and irregularity of a signal [16]. It is the result of a methodology that seeks to quantify the chaotic and unpredictable nature of a signal. Because sEMG can be described as linear enveloped, Gaussian distribution [8], the signal itself can be very chaotic and unpredictable. This suggests that complexity measures may provide new insights into understanding the mechanisms behind neuromuscular firing, particularly how those mechanisms change over time.

Aging is a normal process that results in morphological changes affecting performance capabilities particularly in the neuromuscular systems. The aging process includes denervation of Type-II fibers converting them to Type-I fibers [35,40,43], hypothetically decreasing the variability of the spectral content as Type-II fibers have a higher firing rate vs Type-I fibers. This hypothesis has been examined in the literature with use of complexity measures. Age-related changes to sEMG complexity has been demonstrated for upper and lower extremity musculature [30,32–34,42,55].Arujunan evaluated complexity of the biceps brachii during isometric contractions both experimentally [30] and through modeling [32]. In both instances the authors determined that the older adults had a reduction in complexity of the sEMG when compared to the younger adults. The authors attribute the reduction in complexity specifically to the reduction in the ratio of Type-II to Type-I fibers and to the reduction in total number of muscle fibers. Ao [33] found similar results when examining biceps and triceps function in stroke-affected and unaffected subjects. Age-matched control subjects had lower complexity values vs younger adults. Like Arujunan, the authors attributed these differences to reduction in complexity to a reduction in the number of active motor units along with their respective firing rates in the biceps brachii. Analyses of lower body musculature have produced different results.

Piasecki [42] examined age-related changes in the vastus lateralis of older and young men. They determined that for the vastus lateralis, older adults had higher complexity values than young adults when analyzing sEMG data collected during held isometric contractions at 25% of MVC. This was observed even though many of the expected age-related changes were evident including, reduction in number of motor units, decreased motor unit potential, and reduced firing rates. Dela [34] assessed complexity of the gastrocnemius during a walking task. The authors determined that older adults had greater complexity compared to young adults, though they did not comment directly on how morphological changes were affecting complexity. Kang [55] evaluated muscular complexity with sample entropy for muscle activity from the vastus lateralis, biceps femoris, gastrocnemius, and tibialis anterior during a walking task. The vastus lateralis, biceps femoris, and tibialis anterior had lower complexity values in older adults vs young adults, while the gastrocnemius had higher complexity values in older adults [55]. The higher complexity for the soleus and gastrocnemius lateralis in the current study are in agreement with the results reported by Kang, as they are both part of the triceps surae group. As noted above, the higher complexity values across windows is likely the result of age-related declines in fatigue levels during older individuals' performance of held maximal isometric contractions [52,53,56].

Kang [55] provides three potential reasons for the higher complexity in the gastrocnemius of older adults. The first reason relates to changes in general activation patterns involving gait due to changes in hip and ankle moments, which have also been substantiated in fall related research. Older adults have modified balance recovery techniques compared to younger adults affecting gastrocnemius and tibalis anterior activation [57–61]. The second reason relates to the increase in neuromuscular noise associated with aging in combination with decreased motor drive. Roos [62] notes that neuromuscular noise increases as one ages. Factors include decreasing number of motor units, decreasing size of motor units, propioceptor deterioration, conduction velocity decrease, and deterioration of muscle spindle function. When increased neuromuscular noise is combined with less motor drive, Kang [55] explains the entropy analysis may be dominated by the noise portion. This could also explain the similarity between the gastrocnemius complexity profile and the sample entropy of white noise [34,55]. The third reason for increased complexity in older adults was longer burst activation from walking. Kang [55] measured the time a muscle spent "on" vs "off', and found that higher "on" values corresponded with higher complexity. This effect was noticed in the gastrocnemius for the older adults. Kang [55] speculate that the increased complexity is due to activation patterns in the gastrocnemius becoming similar to that of white noise. Changes in activation patterns could be a potential reason for higher complexity in older adults in our paper.

#### 4.3.2. CSB-AC vs sample entropy

The results of our paper indicate that CSB-AC returns greater complexity values than sample entropy. Four of the five muscle groups yielded statistically significant differences between the two analysis methods. These findings demonstrate that the intensity dynamics methodology of CSB-AC is capturing more of the unpredictability and irregularity of the signal than sample entropy methods. It may be argued that the higher complexity between methods may be associated to high influx of noise within the measurement method itself; however, this is not the case as CSB-AC specifically examines the overall signal size as it determines specific points in time that are associated with the location of maximum intensity.

The mathematical process of CSB-AC incorporates a significant amount of reduced data points in an order of magnitude of a 1000x reduction per spectral band. The use of the wavelet intensity filtering (spectral band) on the EMG signal, which only accounts for the maximum intensity (Activation), is thus extracting key motor recruitment patterns and only preserving the temporal components needed for

characterizing the statistical variation between the two cohort recruitment patterns. The classical techniques apply the entropic method to the entire time domain signal, in which case the key activations within the EMG are washed out by overlapping or embedded intensities of other spectral bands. The novel method overcomes this problem by applying the wavelet intensity filtering before applying sample entropy, preserving both temporal and spectral content. This provides us with more available information when analyzing and evaluating the complexity of the sEMG that is not possible by just using classical techniques such as sample entropy. This can be seen in Fig. 1, where the EMG Intensity During maximum activation (in blue with dots indicting maximums) have additional colored x's on the trace indicting the presence of embedded or hidden spectral intensity band activation. The resulting points indicate the importance of motor recruitment patterns that would otherwise remain unnoticed using classical complexity measures. The strength of CSBAC over classical complexity measures is more evident if we revisit Kang's [55] explanation for increased complexity in older adults. The authors hypothesize that activation patterns of the gastrocnemius are similar to that of white noise, leading to the increased complexity. This interpretation is hindered by their use of sample entropy. In theory, CSB-AC should not be less affected by neuromuscular noise, which would allow researchers to discount it in their analysis. Therefore, this method provides novel insight into the intricacies of neuromuscular dynamics not yet presented in the literature. Although we cannot determine what underlies the difference in complexities between the two methods, we have presented observations and laid the foundational work necessary to rethink motor recruitment dynamics. Using the orchestral analogy, sample entropy can be seen as a patron listening to the symphony, but lacking the ability to distinguish individual elements of the woodwinds, brass, strings, and percussion sections because there are too many instruments or chairs per section. In contrast, during CSB-AC, the full orchestra has been reduced to just the first chairs of each section so the patron can now distinguish the violins from the violas. Once these intricacies are revealed, the errors and the quality of how the chair is playing become more apparent. Thus CSB-AC can better describe the performance of the orchestra or the performance of embedded neuromuscular dynamics. This allows the researcher to ask the next logical question, how important is the violin versus the viola to the overall musical piece?

## 5. Conclusions

This paper lays the foundational work for an innovative technique demonstrating a critically embedded dimension of information within the sEMG signal which will be used to examine neuromuscular firing dynamics in the future. The presented nascent method, CSB-AC, can better uncover muscular activation patterns by preserving the spectral band intensity content and using an entropy approach to measure sEMG signal complexity. We have demonstrated that CSB-AC utilizes strategic motor unit points that are spectrally decomposed within the time series (a factor of 1000x less data points than the original EMG data) to produce significantly greater complexity than sample entropy when assessing sEMG from an isometric contraction. In our experimental test case, CSB-AC revealed that older adults displayed higher levels of complexity than younger adults and that younger adults had a faster rate of decay in complexity. CSB-AC provides a new mathematical approach to deriving the complexity of an electrophysiological signal, such as sEMG, that contains novel information not attainable using current entropic methods. Because CSB-AC reduces the overall signal length when determining the points of activation intensity, it implies that the resulting points have a more critical importance to motor recruitment strategies than previously suggested. There is a need for continued analysis with CSB-AC to allow further understanding of motor recruitment of how motor unit recruitment patterns change due to diseases, injuries and types of contractions. This foundational work will lead to better neuro-muscular prognostics through an enhanced understanding of motor recruitment and firing patterns.

## CRediT authorship contribution statement

**Nicholas J. Napoli:** Conceptualization, Methodology, Formal analysis, Writing – original draft, Software. **Anthony R. Mixco:** Writing – original draft, Formal analysis. **Savannah V. Wooten:** Investigation, Data curation. **Marco Jacopetti:** Investigation, Data curation. **Joseph F. Signorile:** Writing – original draft, Formal analysis, Resources, Writing – review & editing.

## Declaration of competing interest

The authors declare that they have no known competing financial interests or personal relationships that could have appeared to influence the work reported in this paper.

## References


[1] J.V. Basmajian, Muscle fatigue and time-dependent parameters of the surface EMG signal, Muscles Alive Their Functions Revealed by Electromyography, pp. 201–222, 1985.

[2] D. Farina, R. Merletti, Comparison of algorithms for estimation of EMG variables during voluntary isometric contractions, J. Electromyogr. Kinesiol. 10 (5) (2000) 337–349.

[3] V. Von Tscharner, Intensity analysis in time-frequency space of surface myoelectric signals by wavelets of specified resolution, J. Electromyogr. Kinesiol. 10 (6) (2000) 433–445.

[4] J. Wakeling, V. Von Tscharner, B. Nigg, P. Stergiou, Muscle activity in the leg is tuned in response to ground reaction forces, J. Appl. Physiol. (Bethesda, Md. 91 (3) (1985, 2001,) 1307–1317.

[5] J.M. Wakeling, S.A. Pascual, B.M. Nigg, and V. Tscharner, Surface EMG shows distinct populations of muscle activity when measured during sustained submaximal exercise, Eur. J. Appl. Physiol. 86(1) (2001), 40–47.

[6] H. Enders, V. von Tscharner, B.M. Nigg, Analysis of damped tissue vibrations in time-frequency space: A wavelet-based approach, J. Biomech. 45 (16) (2012) 2855–2859.

[7] R. Vetter, J. Schild, A. Kuhn, and L. Radlinger, Discrimination of healthy and postpartum subjects using wavelet filterbank and auto-regressive modelling, in: Proc. of the Intl. Joint Conf. on Biomedical Engineering Systems and Technologies, ser. BIOSTEC 2015, vol. 4, 2015, pp. 132–137.

[8] N. Napoli, A. Mixco, J. Bohorquez, J. Signorile, An EMG comparative analysis of quadriceps during isoinertial strength training using nonlinear scaled wavelets, Hum. Mov. Sci. 40 (2017) 134–153.

[9] T. Jaitner, D. Janssen, R. Burger, and U. Wenzel, Identification of EMG frequncy patterns in running by wavelet analysis and support vector machines, in: Intl. Conf. on Biomechanics in Sports, vol. 28, 2010.

[10] J. Férre, B. Gpfert, J. Slawinski, and C. Tourny-Chollet, Shoulder muscles recruitment during a power backward giant swing on high bar: A Wavelet EMG Analysis, Hum. Movement Sci. 31(2) (2012) 472–485.

[11] S. C. Landry, B. M. Nigg, and K. E. Tecante, Standing in an unstable shoe increases postural sway and muscle activity of selected smaller extrinsic foot muscles, Gait Posture 32(2) (2010) 215–219.

[12] W.J. Armstrong, Wavelet-based intensity analysis of mechanomyographic signals during single-legged stance following fatigue, J. Electromyogr. Kinesiol. 21 (5) (2011) 803–810.

[13] M. Al-Mulla, F. Sepulveda, Novel pseudo-wavelet function for MMG signal extraction during dynamic fatiguing contractions, Sensors 14 (5) (2014) 9489–9504.

[14] T.W. Beck, V. von Tscharner, T.J. Housh, J.T. Cramer, J.P. Weir, M.H. Malek, M. Mielke, Time/frequency events of surface mechanomyographic signals resolved by nonlinearly scaled wavelets, Biomed. Signal Process. Control 3 (3) (2008) 255–266.

[15] Liping Qi, James M. Wakeling, Adam Green, Kirstin Lambrecht, Martin Ferguson-Pell, Spectral properties of electromyographic and mechanomyographic signals during isometric ramp and step contractions in biceps brachii, J. Electromyogr. Kinesiol. 21 (1) (2011) 128–135.

[16] S. Pincus, Approximate entroy as a measure of system complexity, Proc. Natl. Acad. Sci. U.S.A. 88 (6) (1991) 2297–2301.

[17] W. Chen, J. Zhuang, W. Yu, Z. Wang, Measuring complexity using fuzzyen, apen, and sampen, Med. Eng. Phys. 31 (1) (2009) 61–68.

[18] T. Lee, Y. Kim, and P. Sung, Spectral and entropy changes for back muscle fatigability following spinal stabilization exercises, J. Rehab. Res. Dev. 47(2) (2010), 133–142.

[19] X. Zhang, X. Chen, P.E. Barkhaus, P. Zhou, Multiscale entropy analysis of different spontaneous motor unit discharge patterns, IEEE J. Biomed. Health Inf. 17 (2) (March 2013) 470–476.

[20] X. Zhang, D. Wang, Z. Yu, X. Chen, S. Li, P. Zhou, EMG-torque relation in chronic stroke: A novel EMG complexity representation with a linear electrode array, IEEE J. Biomed. Health Inf. 21 (6) (Nov 2017) 1562–1572.

[21] J. Caruso, J. Signorile, A. Perry, M. Clark, and M. Bamman, Time course changes in contractile strength resulting from isokinetic exercise and 2 agonist administration, J. Strength Condit. Res. 11(1)(1997), 8–13.
[22] W. Hopkins, E. Schabort, J. Hawley, Reliability of power in physical performance tests, Sports Med. (Auckland N.Z.) 31 (3) (2001) 211–234.
[23] D. Farina, Counterpoint: Spectral properties of the surface EMG do not provide information about motor unit recruitment and muscle fiber type, J. Appl. Physiol. 105 (5) (2008) 1673–1674.
[24] J.M. Wakeling, D.A. Syme, Wave properties of action potentials from fast and slow motor units of rats, Muscle Nerve 26 (5) (2002) 659–668.
[25] D.M. Pincivero, R.M. Campy, Y. Salfetnikov, A. Bright, A.J. Coelho, Influence of contraction intensity, muscle, and gender on median frequency of the quadriceps femoris, J. Appl. Physiol. 90 (3) (2001) 804–810.
[26] A. Rainoldi, M. Gazzoni, and G. Melchiorri, Differences in myoelectric manifestations of fatigue in sprinters and long distance runners, Physiol. Meas. 29 (3), 331.
[27] N.J. Napoli, M.W. Demas, S. Mendu, C.L. Stephens, K.D. Kennedy, A.R. Harrivel, R. E. Bailey, L.E. Barnes, Measuring the effect of R-peak perturbations caused by corruption on heart rate complexity metrics, Comput. Biol. Med. (2018).
[28] R. Okazaki, T. Takahashi, K. Ueno, K. Takahashi, M. Ishitobi, M. Kikuchi, M. Higashima, Y. Wada, Changes in EEG complexity with electroconvulsive therapy in a patient with autism spectrum disorders: A multiscale entropy approach, Front. Human Neurosci. 9 (2015) 106.
[29] S.A. Akar, S. Kara, F. Latifoglu, and V. Bilgi, Analysis of the complexity measures in the eeg of schizophrenia patients, Intl. J. Neural Syst. 26(02) 2016.
[30] S.P. Arjunan and D.K. Kumar, Age-associated changes in muscle activity during isometric contraction, Muscle and Nerve, 47(4), 545–549.
[31] N.J. Napoli, M. Demas, C.L. Stephens, K.D. Kennedy, A.R. Harrivel, L.E. Barnes, A. T. Pope, Activation complexity: A cognitive impairment tool for characterizing neuro-isolation, Nat. Sci. Rep. 10 (3909) (2020) 1–21.
[32] S.P. Arjunan, K. Wheeler, H. Shimada, and D. Kumar, Age related changes in the complexity of surface EMG in biceps: A model based study, in: 2013 ISSNIP Biosignals and Biorobotics Conf.: Biosignals and Robotics for Better and Safer Living (BRC), Feb 2013, pp. 1–4.
[33] D. Ao, R. Sun, K.-Y. Tong, R. Song, Characterization of stroke- and aging-related changes in the complexity of EMG signals during tracking tasks, Ann. Biomed. Eng. 43 (4) (Apr 2015) 990–1002.
[34] J.B.D. Mark D. Dela and H.G. Kang, Multiscale entropy of EMG during walking in young and older adults, Ann. Biomed. Eng. 990–1002.
[35] R. Merletti, D. Farina, M. Gazzoni, M.P. Schieroni, Effect of age on muscle functions investigated with surface electromyography, Muscle Nerve 25 (1) (2002) 65–76.
[36] J. Kallio, J. Avela, T. Moritani, M. Kanervo, H. Selnne, P. Komi, V. Linnamo, Effects of ageing on motor unit activation patterns and reflex sensitivity in dynamic movements, J. Electromyogr. Kinesiol. 20 (4) (2010) 590–598.
[37] M.R. Roos, C.L. Rice, A.A. Vandervoort, Age-related changes in motor unit function, Muscle Nerve 20 (6) (1997) 679–690.
[38] J.M. Thom, C.I. Morse, K.M. Birch, M.V. Narici, Triceps surae muscle power, volume, and quality in older versus younger healthy men, J Gerontol.: Ser. A 60 (9) (2005) 1111–1117.
[39] I.S. Raj, S.R. Bird, A.J. Shield, Aging and the forcevelocity relationship of muscles, Exp. Gerontol. 45 (2) (2010) 81–90.
[40] Y.C. Jang and H.V. Remmen, Age-associated alterations of the neuromuscular junction, Exp. Gerontol. 46(2) (2011), 193–198, proc. of the Tenth Intl. Symposium on Neurobiology and Neuroendocrinology of Aging.
[41] J.A. Faulkner, L.M. Larkin, D.R. Claflin, S.V. Brooks, Age-related changes in the structure and function of skeletal muscles, Clin. Exp. Pharmacol. Physiol. (2007).
[42] M. Piasecki, A. Ireland, D. Stashuk, A. Hamilton-Wright, D.A. Jones, and J.S. McPhee, Age-related neuromuscular changes affecting human vastus lateralis, J. Physiol. 594(16), 4525–4536.
[43] W. Mitchell, P. Atherton, J. Williams, M. Larvin, J. Lund, M. Narici, Sarcopenia, dynapenia, and the impact of advancing age on human skeletal muscle size and strength; a quantitative review, Front. Physiol. 3 (2012) 260.
[44] M. Narici, C. Maganaris, and N. Reeves, Myotendinous alterations and effects of resistive loading in old age, Scand. J. Med. Sci. Sports 15(6), 392–401.
[45] J.F. Signorile, D. Sandler, F. Ma, S. Bamel, D. Stanziano, W. Smith, B.A. Roos, L. Sandals, The gallon-jug shelf-transfer test: An instrument to evaluate deteriorating function in older adults, J. Aging .Phys. Activity 15 (1) (2007) 56–74.
[46] E. Criswell, Crams Introduction to Surface Electromyography, Jones and Bartlett Publishers, Boston, MA, 2011.
[47] D.A. Gabriel and G. Kamen, Point:counterpoint comments, J. Appl. Physiol. 105 (2008).
[48] F. Borg, Filter banks and the intensity analysis of EMG, http://arxiv.org/abs/1005.0696, 2010.
[49] D. Lake, J. Richman, M. Griffin, R. Moorman, Sample entropy analysis of neonatal heart rate variability, Am. J. Physiol. 283 (3) (2002) R789–R797.
[50] A. Christie, G. Kamen, Motor unit firing behavior during prolonged 50% mvc dorsiflexion contractions in young and older adults, J. Electromyogr. Kinesiol. 19 (4) (2009) 543–552.
[51] S. Rubinstein, G. Kamen, Decreases in motor unit firing rate during sustained maximal-effort contractions in young and older adults, J. Electromyogr. Kinesiol. 15 (6) (2005) 536–543.
[52] I.R. Lanza, D.W. Russ, J.A. Kent-Braun, Age-related enhancement of fatigue resistance is evident in men during both isometric and dynamic tasks, J. Appl. Physiol. 97 (3) (2004) 967–975.
[53] K.M. Chan, A.J. Raja, F.J. Strohschein, K. Lechelt, Age-related changes in muscle fatigue resistance in humans, Can. J. Neurol. Sci. 27 (3) (2000) 220–228.
[54] J. Lexell, K. Henriksson-Larsen, B. Winblad, M. Sjostrom, Distribution of different fiber types in human skeletal muscles: effects of aging studied in whole muscle cross sections, Muscle Nerve 6 (8) (1983) 588–595.
[55] H.G. Kang and J.B. Dingwell, Differential changes with age in multiscale entropy of electromyography signals from leg muscles during treadmill walking, PLOS ONE 11(8), 2016.
[56] S.C. Webber, M.M. Porter, P.F. Gardiner, Modeling age-related neuromuscular changes in humans, Appl. Physiol. Nutr. Metab. 34 (4) (2009) 732–744.
[57] Y.-H. Chu, P.-F. Tang, H.-Y. Chen, C.-H. Cheng, Altered muscle activation characteristics associated with single volitional forward stepping in middle-aged adults, Clin. Biomech. 24 (9) (2009) 735–743.
[58] E.T. Hsiao-Wecksler, Biomechanical and age-related differences in balance recovery using the tether-release method, J. Electromyogr. Kinesiology 18 (2) (April 2008) 179–187.
[59] D. Mackey, S. Robinovitch, Mechanisms underlying age-related differences in ability to recover balance with the ankle strategy, Gait Posture 23 (2006) 59–68.
[60] S. Okada, Age-related differences in postural control in humans in response to a sudden deceleration generated by postural disturbance, Eur. J. Appl. Physiol. 85 (2001) 10–18.
[61] A. Mixco, M. Reynolds, B. Tracy, R.F. Reiser II, Aging-related cocontraction effects during ankle strategy balance recovery following tether release in women, J. Mot. Behav. 44 (1) (2012) 1–11.
[62] Paulien E. Roos, Jonathan B. Dingwell, Influence of simulated neuromuscular noise on movement variability and fall risk in a 3d dynamic walking model, J. Biomech. 43 (15) (2010) 2929–2935.